15

NMR Studies of Emulsions with Particular Emphasis on Food Emulsions

Balin Balinov
Amersham Health, Oslo, Norway

Francois Mariette
Cemagref, Rennes, France

Olle Söderman
University of Lund, Lund, Sweden

I. INTRODUCTION

Very early in the development of colloid science, emulsions received considerable attention. This is due to the fact that emulsions are of great fundamental as well as technical importance. They occur in a multitude of situations ranging from the extraction of crude oil to various food products. Therefore, it is not surprising that the practical knowledge about emulsions is quite extensive. People engaged in the production generally know how to produce emulsions with desired properties such as droplet-size distributions and shelf-life. The same level of empirical knowledge is at hand for the opposite process of breaking an emulsion. When it comes to the basic scientific understanding of emulsions, we are a little worse off. It is quite clear that several fundamental properties of emulsions, such as what factors determine the stability of emulsions, what is the importance of the properties of the continuous phase, and so on, are not fully understood. To some extent, we also lack or have not yet applied suitable techniques in the study of emulsions.

The majority of emulsions are stabilized by surfactants and Bancroft, one of the pioneers in emulsion science, realized that the stability of an emulsion was related to the properties of the surfactant film. This insight has become important during the latter years, when attempts have been made to draw on the rather detailed and profound understanding that today exists about bulk surfactant systems in the description of emulsions (1). This high level of understanding about bulk surfactant systems stems not the least from the application of modern physicochemical techniques such as scattering methods and nuclear magnetic resonance (NMR). It seems reasonable to expect that the application of these techniques to emulsion systems would lead to an increased basic understanding of central emulsion properties.

In this contribution, we will attempt to show how NMR can be used to study various emulsion systems and how NMR may be used in emulsion applications. We focus in particular on food emulsions, which, by their very nature, cover a very wide area in practical applications. One finds "semi-solid" varieties such as margarine and butter as well as liquid ones such as milk, sauces, dressings, and various beverages. In addition, food emulsions also include an array of products that contain both solids and/or gases in addition to two liquid phases such as in ice cream. Because of the complexity in their chemical composition and their heterogeneous structure, the use of NMR techniques in the study of food emulsions are up until now relatively limited. This is in contrast to the many studies dealing with biopolymers and their structure modification induced by food processing. The first applications of NMR to food emulsions were in the determination of solid-fat content and emulsion composition. These methods are based on the relative NMR signal intensities. Somewhat surprisingly, the relaxation time variation as a function of fat and/or water phase structure and composition has received little attention. Since the development of new benchtop NMR spectrometers, new applications using both relaxation time parameters and self-diffusion coefficient have been suggested and introduced.

We first discuss the NMR technique as such, with special emphasize on features important for the study of emulsions. Subsequently, we treat some important examples of how NMR can be used to obtain important information about central aspects of emulsions, in general, and food emulsions, in particular.

II. THE NMR TECHNIQUE

A. Fundamentals

Nuclear magnetic resonance is a spectroscopic technique and as such it is very well suited for investigations of topics such as molecular arrangements

and molecular dynamics. NMR has gone through a dramatic development over the last decades. For this reason, there are numerous monographs treating many different aspects of the method (2–4). Here, we will attempt to introduce the technique from the point of view of emulsion science.

Nuclear magnetic resonance spectroscopy is based on the fact that some nuclei possess a permanent nuclear magnetic moment. When placed in an external magnetic field, they take a certain well-defined state, which correspond to distinct energy levels. Transitions between neighboring energy levels take place due to absorption of electromagnetic radiation at radio-frequencies. In NMR, the signal is obtained by a simultaneous excitation of all transitions with radio-frequency pulses, followed by detection of the irradiation emitted as the system returns to the equilibrium state. The recorded free-induction decay (FID) may be used as such, but Fourier transformation of the time-resolved FID is usually performed to obtain the NMR spectrum.

Modern NMR spectrometers, operating at 500–800 MHz for protons, have a high resolution that allows one to identify up to several hundreds of lines in a complex NMR spectrum. In most cases, only a limited number of lines are used to obtain the information needed. In some applications, the spectral resolution is not a necessary step in the data analyses and the information may be obtained from the time dependence of the amplitude of the FID. The FID reflects all of the nuclei of a given type (e.g., protons) and is used to obtain information on the average relaxation phenomena of the nuclei of interest. For this type of signal detection, 10–20-MHz NMR spectrometers for protons is an option suitable for many industrial applications.

Nuclear magnetic resonance is a very versatile spectroscopic technique for three main reasons. (1) It is not a destructive technique. Thus, the system may be studied without any perturbation that influences the outcome and interpretations of the measurements. The system can be characterized repeatedly with no time-consuming sample preparations in between runs. (2) There are a large number of spectroscopic parameters that may be determined by NMR relating to both static and dynamic aspects of a wide variety of systems. (3) A large number of atomic nuclei carry nuclear spins, and for essentially any element in the periodic table, it is possible to find at least one suitable nucleus. This has the important consequence that for systems that show local segregation (such as surfactant and emulsion systems), it is possible to investigate different domains of the microheterogeneous system by studying different nuclei.

The most commonly used nucleus in NMR is ^{1}H, but also ^{13}C, ^{19}F, ^{23}Na and ^{31}P are of importance. These nuclei are naturally occurring isotopes and need not be inserted chemically. Another very useful nucleus

is ^2H; however, the natural abundance of this species is, in general, too small to allow for reasonable measuring times. Therefore, this nucleus is usually inserted by chemical labeling. This can, in fact, be used to an advantage because the ^2H nucleus can be directed to a particular part of the molecule, hence making it possible to investigate different parts of a molecule.

It is convenient to divide the parameters obtained from NMR spectra into dynamic and static parameters.

B. Static Parameters

The static parameters are obtained from the observed resonance frequencies. The general frequency range where a particular nucleus shows a spectroscopic line is determined by the magnetogyric ratio, which is a nuclear property without chemical interest. However, the precise value of the resonance frequency is determined by molecular properties. For isotropic systems, the two most important parameters determining the resonance frequency is the chemical shift and the scalar spin–spin coupling.

The chemical shift is determined by the screening due to the electrons in the vicinity of the investigated nucleus. This, in turn, is determined mainly by the primary chemical structure of the molecule but also other factors such as hydrogen-bonding, conformation, and the polarity of the environment influence the chemical shift. In systems with local segregation, such as emulsions, this has the consequence that one may observe two separate signals from the same molecule if it resides in two different environments. This occurs if the exchange of the molecule between the two environments is slow on the relevant timescale, which is given by the inverse of the shift difference between the two environments. This feature of the experiment gives us the possibility to investigate the distribution of molecules and exchange rates in microheterogeneous systems.

The scalar coupling is exclusively of intramolecular origin and of little importance in emulsion systems.

Another static parameter of importance is the integrated area under a given peak. This quantity is proportional to the number of spins contributing to a given peak, and hence (relative) concentrations can be determined. This, as will be shown in Sect. VI, has some important applications in emulsion science.

C. Dynamic Parameters

Dynamic processes on the molecular level influence the nuclear spin system by rendering the spin Hamiltonian time dependent. Depending on the relation between the characteristic times of the molecular motions, τ_c, and the

strength of the modulated interaction, ω_I (expressed in frequency units), one can identify different regimes.

For slow motions, when $\tau_c\omega_I \gg 1$, the system is in the solid regime and ω_I contributes to the resonance frequencies observed. This is the situation encountered in anisotropic liquid crystals, where the NMR spectra are usually dominated by static effects.

In the other extreme, when $\tau_c\omega_I \ll 1$, the phenomenon of motional narrowing occurs. Here, the spin relaxation is characterized by a limited number of time constants, the most readily observed are the longitudinal, T_1, and transverse, T_2, relaxation times. The first of these characterizes the decay of the M_z magnetization to equilibrium and the second characterizes the return of the $M_{x,y}$ magnetization to equilibrium (where M_z is perpendicular to the polarizing magnetic field and $M_{x,y}$ lies in a plane perpendicular to M_z). Measurements of the relaxation times require that the sample is perturbed by various pulse sequences. The one most often used for measuring T_1 is the inversion recovery sequence (or variations of it), and different echo sequences are usually used for measuring T_2.

For the case when $\tau_c\omega_I \approx 1$, the shape of the NMR spectral line is strongly affected by the characteristic features of the molecular motions.

We shall make two remarks concerning features, which are peculiar to the topic of NMR and emulsions. The first deals with the fact that an emulsion system may actually contain molecules that fulfill more than one of the motional regimes described earlier. Consider, for instance, molecules in the continuous phase. For them, the condition $\tau_c\omega_I \ll 1$ holds. For molecules residing at the interface between the two liquids of the emulsion, the situation may be different, and depending on the size of the emulsion droplet, they may experience any of the three time domains described earlier.

Our second remark deals with the effect of diamagnetic susceptibility variations. In heterogeneous structures, the magnetic field is perturbed in the vicinity of regions of differing susceptibilities. As a consequence, the random motions of the molecules in this spatially varying magnetic field induces relaxation effects. T_1 and T_2 relaxation require fluctuations at the Larmor frequency, whereas, in addition, T_2 relaxation is also sensitive to slower fluctuations. Because the fluctuations brought about by diffusion in the locally varying field typically occur with rates, which are slower than the Larmor frequencies, $T_2 \ll T_1$ for this effect. Peculiar to systems with spherical structures, such as reasonably dilute emulsions, is that the gradient of the magnetic field *inside* the droplet is not affected. Thus, the above-described effect only operates for the continuous phase, which can be used to identify whether an emulsion is of the oil-in-water or water-in-oil type in a straightforward manner (5).

D. Measurement of Self-Diffusion

A very important dynamic molecular process is that of the transport of molecules due to thermal motion. This can conveniently be followed by the NMR pulsed field gradient (PFG) method. Because this approach has been of particular importance in the field of microheterogenous surfactant systems, in general, and in emulsion systems, in particular, we will spend some time introducing this application of NMR. The technique has recently been described in a number of review articles (cf. Refs. 2 and 6–8), so here we will merely state that the technique requires no addition of probes, thus avoiding possible disturbances that addition of probes may cause, and that it gives component resolved self-diffusion coefficients with great precision in a minimum of measuring time. The main nucleus studied is the proton, but other nuclei, such as Li, F, Cs, and P, are also of interest.

The method monitors transport over macroscopic distances (typically in the micrometer regime). Therefore, when the method is used to study colloidal systems, the determined diffusion coefficients reflect aggregate sizes and obstruction effects for colloidal particles. This is the origin of the success the method has had in the study of microstructures of surfactant solutions and also forms the basis of its applications to emulsion systems. We expect that the PFG method will also be increasingly important in the study of emulsion systems and, therefore, we will discuss the method in some detail, with particular focus on its application to emulsions.

The fact that the information is obtained without the need to invoke complicated models, as is the case for the NMR relaxation approach, is particularly important. In this context, it should be stressed that the PFG approach measures the self-diffusion rather than the collective diffusion coefficient, which is measured by, for instance, light-scattering methods.

In its simplest version, the method consists of two equal and rectangular gradient pulses of magnitude g and length δ, one on either side of the 180° radio-frequency(rf)-pulse in a simple Hahn echo experiment. For molecules undergoing free (Gaussian) diffusion characterized by a single diffusion coefficient of magnitude D, the echo attenuation due to diffusion is given by (9,10)

$$E(\Delta, \delta, g) = E_0 \exp\left[-\gamma^2 g^2 \delta^2 \left(\Delta - \frac{\delta}{3}\right) D\right] \tag{1}$$

where Δ represents the distance between the leading edges of the two gradient pulses, γ is the magnetogyric ratio of the monitored spin, and E_0

denotes the echo intensity in the absence of any field gradient. By varying either g, δ, or Δ (while at the same time keeping the distance between the two Rfpulses constant), D can be obtained by fitting Eq. (1) to the observed intensities.

As mentioned earlier, the key feature of PFG diffusion experiments is the fact that the transport of molecules is measured over a time Δ, which we are free to choose at our own will in the range of from a few milliseconds to several seconds. This means that the length scale over which we are measuring the molecular transport is in the micrometer regime for low-molecular-weight liquids. When the molecules experience some sort of boundary with regard to their diffusion during the time Δ, the molecular displacement is lowered as compared to free diffusion, and the outcome of the experiment becomes drastically changed (2,11,12).

This situation applies to the case of restricted motion inside an emulsion droplet. In this case, the molecular displacements cannot exceed the droplet size, which indeed often is in the micrometer regime. Until recently, no analytical expressions that describe the echo decay in restricted geometries for arbitrary gradient pulses have been available. However, Barzykin(13) and Codd and Callaghan(14) have developed two approaches that work for arbitrary gradient pulses. This is an important step and will undoubtedly lead to an increased applicability of the method. Because the application of these approaches are somewhat numerically cumbersome and PFG work performed up until now mainly rely on one of two approximate schemes, we will describe these schemes below.

In one of these, one considers gradient pulses, which are so narrow that no transport during the pulse takes place. This has been termed the short gradient pulse (SGP) (or narrow gradient pulse, NGP) limit. This case leads to a very useful formalism whereby the echo attenuation can be written as (2)

$$E(\delta, \Delta, g) = \iint \rho(\mathbf{r}_0) P(\mathbf{r}_0|\mathbf{r}, \Delta) \exp[i\gamma g\delta(\mathbf{r} - \mathbf{r}_0)]\, d\mathbf{r}\, d\mathbf{r}_0 \tag{2}$$

where $P(\mathbf{r}_0|\mathbf{r}, \Delta)$ is the propagator, which gives the probability of finding a spin at position $\mathbf{r}$ after a time Δ if it was originally at position $\mathbf{r}_0$.

As discussed by Kärger and Heink(15) and Callaghan (2), Eq. (2) can be used to obtain the displacement profile, which is the probability for a molecule to be displaced dz during Δ in the direction of the field gradient, irrespective of its starting position. Modern NMR spectrometers are capable of producing gradient pulses with durations less than 1 ms and with

strengths around 10 T/m. Under these conditions, the SGP limit is often valid. The challenge is to design $E(\delta, \Delta, g)$ experiments that are sensitive to a particular type of motion in a system of interest. The study topics include free diffusion in the continuous phase in emulsions, restricted diffusion inside emulsion droplets, molecular exchange between emulsion droplets in highly concentrated emulsions, or drug release from emulsion droplets. Some of those examples will be considered in this chapter.

For the case of free diffusion, $P(\mathbf{r}_0|\mathbf{r}, \Delta)$ is a Gaussian function, and if this form is inserted in Eq. (2), Eq. (1) with the term $\Delta - \delta/3$ replaced with Δ is obtained, which is the SGP result for free diffusion. For cases other than free diffusion, alternate expressions for $P(\mathbf{r}_0|\mathbf{r}, \Delta)$ have to be used. Tanner and Stejskal (16) solved the problem of reflecting planar boundaries; however, the case of interest to us in the context of emulsion droplets, (i.e. that of molecules confined to a spherical cavity of radius R) was presented by Balinov et al. (17). The result is

$$\begin{aligned} E(\delta, \Delta, g) = & \frac{9[\gamma g \delta R \cos(\gamma g \delta R) - \sin(\gamma g \delta R)]^2}{(\gamma g \delta R)^6} \\ & + 6(\gamma g \delta R)^2 \sum_{n=0}^{\infty} \left[j_n'(\gamma g \delta R) \right]^2 \\ & \times \sum_m \frac{(2n+1)\alpha_{nm}^2}{\alpha_{nm}^2 - n^2 - n} \exp\left(-\frac{\alpha_{nm}^2 D \Delta}{R^2} \right) \frac{1}{\left[\alpha_{nm}^2 - (\gamma g \delta R)^2 \right]^2} \end{aligned} \quad (3)$$

where $j_n(x)$ is the spherical Bessel function of the first kind and α_{nm} is the m^{th} root of the equation $j_n'(\alpha) = 0$. D is the bulk diffusion of the entrapped liquid, and the rest of the quantities are as defined earlier. The main point to note about Eq. (3) is that the echo amplitudes do indeed depend on the radius, and thus the droplet radii can be obtained from the echo decay for molecules confined to reside in a sphere, provided that the conditions underlying the SGP approximation are met.

The second approximation used is the so-called Gaussian phase distribution. Originally introduced by Douglass and McCall (18), the approach rests on the approximation that the phases accumulated by the spins on account of the action of the field gradients are Gaussian distributed. Within this approximation and for the case of a steady gradient, Neuman (19) derived the echo attenuation for molecules confined within a sphere, within a cylinder and between planes. For spherical geometry, Murday and Cotts (20) derived the equation for pulsed field gradients in the Hahn echo experiment described earlier.

The result is

$$\begin{aligned}
&\ln[E(\delta,\Delta,g)] \\
&\quad = -\frac{2\gamma^2 g^2}{D}\sum_{m=1}^{\infty}\frac{\alpha_m^{-4}}{\alpha_m^2 R^2 - 2} \\
&\qquad \times\left(2\delta - \frac{2+\exp\left[-\alpha_m^2 D(\Delta-\delta)\right]-2\exp\left(-\alpha_m^2 D\delta\right)}{\alpha_m^2 D}\right) \\
&\qquad -\frac{2\exp\left(-\alpha_m^2 D\Delta\right)+\exp\left[-\alpha_m^2 D(\Delta+\delta)\right]}{\alpha_m^2 D}
\end{aligned} \tag{4}$$

where α_m is the m^{th} root of the Bessel equation $(1/(\alpha R))J_{3/2}(\alpha R) = J_{5/2}(\alpha R)$. Again, D is the bulk diffusion coefficient of the entrapped liquid.

Thus, we have at our disposal two equations with which to interpret PFG data from emulsions in terms of droplet radii, neither of which are exact for all values of experimental and system parameters. As the conditions of the SGP regime are technically demanding to achieve, Eq. (4) (or limiting forms of it) have been used in most cases to determine the droplet radii. A key question is then under what conditions Eq. (4) is valid. That it reduces to the exact result in the limit of $R\to\infty$ is easy to show and also obvious from the fact that we are then approaching the case of free diffusion, in which the Gaussian phase approximation becomes exact.

Balinov et al. (17) performed accurate computer simulations aimed at further testing its applicability over a wide range of parameter values. An example is shown in Fig. 1. The conclusion reached in Ref. 17 was that Eq. (4) never deviates by more than 5% in predicting the echo attenuation for typically used experimental parameters. Thus, it is a useful approximation and we will use it in Section III.

As pointed out earlier, the NMR echo amplitude E depends on the droplet's radius, which can be estimated by measuring E at different durations of δ and/or magnitudes g of the pulsed gradient. Typical echo attenuation profiles, generated by using Eq. (4), are presented in Fig. 2, which demonstrates the sensitivity of the NMR self-diffusion experiment to resolve micrometer droplet sizes.

We end this section by noting that the above discussion applies to the situation when the dispersed phase cannot exchange between droplets or between the droplets and the continuous medium (at least on the relevant timescale). This is the case for most emulsions. However, for some concentrated emulsions, this is not necessarily the case and the molecules of the dispersed phase may actually exchange between droplets during the characteristic time of the measurement. This leads to special effects, which will be discussed in Section III.

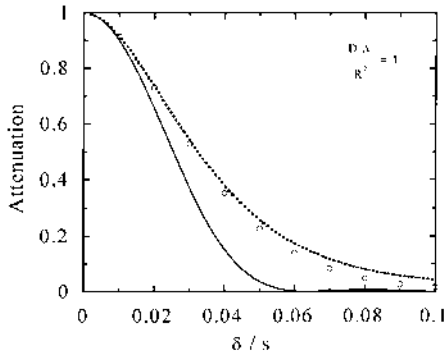

Figure 1 Results of a simulation of the diffusion of water molecules inside an emulsion droplet of radius R, given as the echo amplitude, versus the duration δ of the field gradient pulse. The ratio $D\Delta/R^2$ is 1. The dotted line is the prediction of the Gaussian phase approximation [Eq. (4)], whereas the solid line is the prediction of the SGP [Eq. (3)]. (Adapted from Ref. 17.)

III. STUDIES OF DIFFUSION AND FLOW IN EMULSIONS

A. Determination of Emulsion Droplet Radii by Means of the NMR Diffusometry Method

As pointed out earlier, the echo attenuation curve for the PFG experiment when applied to molecules entrapped in an emulsion droplet is a signature of the size of the emulsion droplet (cf. Fig. 2). As a consequence, droplet sizes can be determined by means of the PFG experiment.

The NMR sizing method, which was apparently first suggested by Tanner in Ref. 10 has been applied to a number of different emulsions ranging from cheese and margarines to crude oil emulsions (21–27).

When applied to a real emulsion one has to consider the fact that the emulsion droplets in most cases are polydisperse in size. This effect can be accounted for if the molecules confined to the droplets are in a slow-exchange situation, meaning that their lifetime in the droplet must be longer than Δ. For such a case, the echo attenuation is given by

$$E_{poly} = \frac{\int_0^\infty R^3 P(R) E(R)\, dR}{\int_0^\infty R^3 P(R)\, dR} \tag{5}$$

where $P(R)$ represents the droplet size distribution function and $E(R)$ represents the echo attenuation according to Eq. (4) [or, within the SGP approximation, Eq. (3)] for a given value of R.

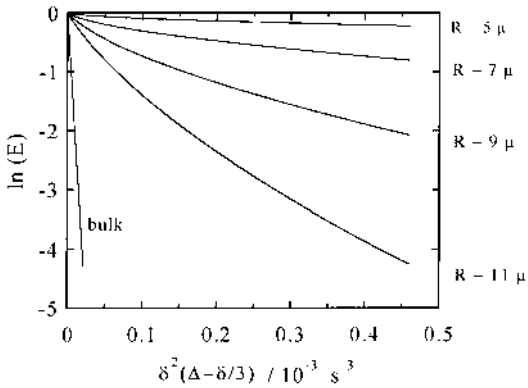

Figure 2 The echo attenuation as a function of $\delta^2(\Delta-\delta/3)$ for different radii of emulsion droplets [according to Eq. (4)] with $\Delta = 0.100$ s, $\gamma g = 10^7$ rad/m/s, and $D = 2 \times 10^{-9}\,\mathrm{m}^2/\mathrm{s}$.

The principle goal is to extract the size distribution function $P(R)$ from the experimentally observed ($E(\delta, \Delta, g)$) (henceforth referred to as E) profiles. Two approaches have been suggested. In the first, one assumes the validity of a model size distribution with a given analytical form (26,27), whereas in the second, the size distribution which best describes the observed experimental E profiles is obtained without any assumption on the form of the size distribution (28,29).

A frequently used form for the size distribution (26,27) is the log-normal function as defined in Eq. (6), as it appears to be a reasonable description of the droplet size distribution of many emulsions:

$$P(R) = \frac{1}{2R\sigma\sqrt{2\pi}} \exp\left[-\frac{(\ln 2R - \ln d_0)^2}{2\sigma^2}\right] \tag{6}$$

In addition, it has only two parameters, which makes it convenient for modeling purposes. In Eq. (6), d_0 represents the diameter median and σ is a measure of the width of the size distribution.

To illustrate the method and discuss its accuracy, we will use as an example some results for margarines (low-calorie spreads) (21). This system highlights some of the definite advantages of using the NMR method to determine emulsion droplet sizes, because other nonperturbing methods hardly exist for these systems.

Given in Fig. 3 is the echo decay for the water signal of a low-calorie spread containing 60% fat. These systems are w/o emulsions and as can be

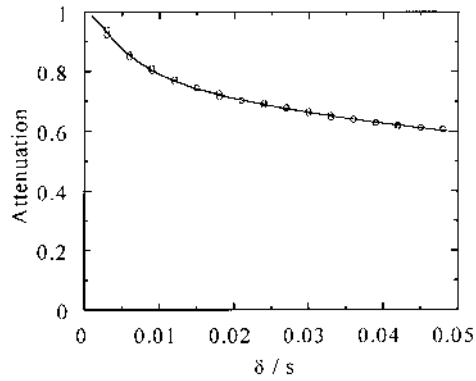

Figure 3 Echo intensities for the entrapped water in droplets formed in a low-calorie spread containing 60% fat versus δ. The solid line corresponds to the predictions of Eqs. (4)–(6). The results from the fit are $d_0 = 0.82\,\mu m$ and $\sigma = 0.72$. (Adapted from Ref. 21.)

seen the water molecules do experience restricted diffusion (in the representation of Fig. 3, the echo decay for free diffusion would be given by a Gaussian function). Also given in Fig. 3 is the result of fitting Eqs. (4)–(6) to the data. As is evident, the fit is quite satisfactory and the parameters of the distribution function obtained are given in the figure caption. However, one might wonder how well determined these parameters are, given the fact that the equations describing the echo attenuation are quite complicated. To test this matter further, Monte Carlo calculations were performed in Ref. 21. Thus, random errors were added to the echo attenuation and the least squares minimization was repeated 100 times, as described previously (30). A typical result of such a procedure is given in Fig. 4. As can be seen in Fig. 4 the parameters are reasonably well determined, with an uncertainty in R (and σ, data not shown) of about $\pm 15\%$.

In the second approach, Ambrosone et al. (28,29) have developed a numerical procedure based on a solution of the Fredholm integral equation to resolve the distribution function $P(R)$ without prior assumptions of its analytical type. The method involves the selection of a generating function for the numerical solution, which may not be trivial in some cases. The method was tested by computer simulation of E for a hypothetical emulsion with a bimodal droplet size distribution (31). Figure 5 shows the reconstruction of the true droplet size distribution from the synthesized E data.

Creaming or sedimentation of emulsions with droplet sizes above 1 μm cause some experimental difficulty because of the change of the total amount of spins in the NMR active volume of the sample tube during the

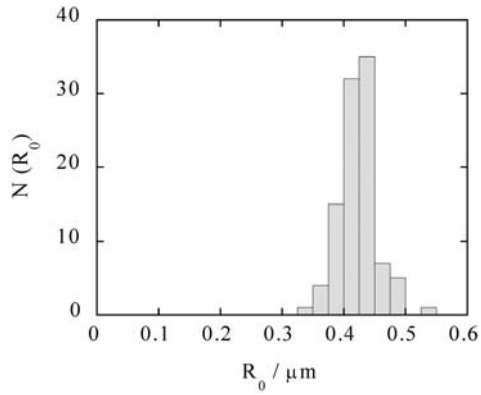

Figure 4 A Monte Carlo error analysis of the data in Fig. 3. The value of the parameter d_0 in Eq. (6) is $d_0 = 0.82 \pm 0.044\,\mu m$ (note that $R_0 = d_0/2$ is plotted). (Adapted from Ref. 21.)

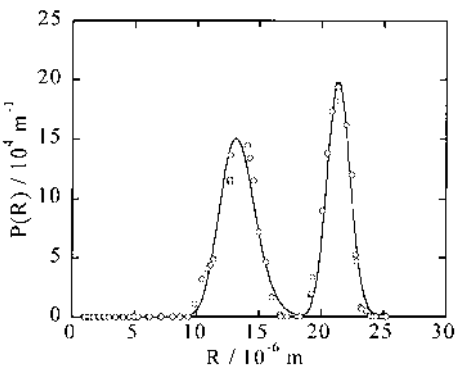

Figure 5 Determination of the size distribution function in the case of a bimodal distribution. The solid line represents the "true" volume fraction distribution function. The dots represents its values evaluated from the generated NMR data. (Adapted from Ref. 31.)

experiment. This can be accounted for by extra reference measurements with no gradient applied before and after each NMR scan at a particular value of δ or g. In addition, such reference measurements may provide information on the creaming rate, which is a useful characteristic of emulsions. Creaming or sedimentation is not a problem in the study of most food emulsions (such as low-calorie spreads) and highly concentrated emulsions.

Emulsion droplet sizes in the range from 1 μm up to 50 μm can be measured with rather modest gradient strengths of about 1 T/m. Note that the size determination rests on determining the molecular motion of the dispersed phase, so the method cannot be applied to dispersed phases with low molecular mobility. In practice, oils with self-diffusion coefficients above $10^{-12}\,m^2/s$ are required for sizing of o/w emulsion. Of course, w/o emulsions with most conceivable continuous media can be sized.

Emulsion droplets below 1 μm in size can often be characterized by the Brownian motion of the droplet as such (exceptions are concentrated emulsions or other emulsions where the droplets do not diffuse). This is the approach taken in the study of microemulsion droplets, where the diffusion behavior of the solubilized phase is characterized by the droplets (Gaussian) diffusion.

In conclusion, we summarize the main advantages of the NMR diffusion method as applied to emulsion droplet sizing. It is nonperturbing, requiring no sample manipulation (such as dilution with the continuous phase), and nondestructive, which means that the same sample may be investigated many times, which is important if one wants to study long-time stability or the effect of certain additives on the droplet size. It requires small amounts of sample (typically on the order of a few 100 mg). Moreover, the total NMR signal from the dispersed phase in emulsions is usually quite intense because of the large amount of spins. This fact allows for rapid measurements with a single scan per δ/g point.

B. Applications of NMR Techniques to Investigate Diffusion and Flow in Food Emulsions

Most of the applications of NMR diffusimetry on food emulsion are focused on the droplet size measurement described earlier. Over the years, several groups have established (21,26,27) the usefulness of the method when applied to margarine and low-calorie spreads (cf. Fig. 3 and 4) and the method is now available on commercial benchtop NMR spectrometers from Bruker, Oxford Instruments, or Universal Systems. However, in the open literature, there are relatively few articles that have been published dealing with droplet sizing of food emulsion. One contribution presents water self-diffusion and fat self-diffusion in cheese (23). Callaghan et al. found no significant difference in the value of the diffusion coefficients between Swiss and cheddar cheese. The water self-diffusion coefficient was about one-sixth of the value of bulk water at 30°C and it was suggested that water diffusion is confined to the protein surface. The self-diffusion of fat was reduced because of restrictions induced by the droplets.

Another study deals with the mobility of lipid contained in bread as a function of water content and temperature (32). The self-diffusion coefficient obtained at 30°C is of the same order as the one measured for the diffusion of lipids in bulk milk fat and was slightly affected by a change in water content (from 6% to 9%). The self-diffusion corresponds to the intrinsic motion within the lipid globule, and the distances probed were too small to allow the molecules to reach the droplet interface.

Because certain NMR experiments are sensitive to motion, flow can be measured with appropriate experimental protocols. These techniques are referred to as NMR velocimetry. The advantage of this technique is that a velocimetry profile or map can be obtained without assumptions of the uniformity of the shear rate. Because many food products exhibit complex non-Newtonian rheological properties, NMR velocimetry across the annular gap of a Couette cell allows for the visualization of nonuniform behavior. For example, the effect of the temperature on the rheology of butter fat and margarine has been studied (33). The results show the effect of the temperature on the heterogeneity of the rheological status of the sample. Moreover, the transition from heterogeneous to homogeneous viscosity as a function of the temperature was dependent on the emulsion composition and structure.

IV. NMR DIFFUSION STUDIES OF CONCENTRATED EMULSIONS

The above discussion applies to the case where the molecules are confined to the droplets on the timescale of the experiment. This is a reasonable assumption for many emulsions and it can in fact be tested by the NMR diffusion method by varying Δ. However, there are some interesting emulsion systems where this is not always the case. These are the so-called highly concentrated emulsions (often termed ''high internal phase ratio'' or ''gel emulsions'') (34,35), which may contain up to (and in some cases even more than) 99% dispersed phase. Here, the droplets are separated by a liquid film, which may be very thin (on the order of 0.1 μm) and which may, in some instances, be permeable to the dispersed phase.

The case when the persistent time of the dispersed phase in the droplet is of the same order of magnitude as Δ is particularly interesting. Under these conditions, one may in some cases obtain one (or several) peak(s) in the plot of the echo amplitudes versus the quantity q (which is defined as $q = \gamma g \delta / 2\pi$). This is a surprising result at first sight, as we are accustomed to observe a monotonous decrease of the echo amplitude with q, but it is actually a manifestation of the fact that the diffusion is no longer Gaussian.

Such peaks can be rationalized within a formalism related to the one used to treat diffraction effects in scattering methods (36), and the analysis of the data may yield important information regarding not only the size of the droplets but also the permeability of the dispersed phase through the thin films as well as the long-term diffusion behavior of the dispersed phase. In Fig. 6, we show the results, which display diffractionlike effects in a concentrated emulsion system. The particular example pertains to a concentrated three-component emulsion based on a nonionic surfactant with the composition $C_{12}E_4/C_{10}H_{22}/H_2O$(1 wt % NaCl) (3/7/90 wt%). The concentrated emulsion was made according to a protocol described in Ref. 37.

The data in Fig. 6 are presented with the value of the quantity q (defined earlier) on the abscissa. This quantity has the dimension of inverse length and it is, in fact, related to the scattering vector used in describing scattering experiments. In fact, the inverse of the value of the position of the peak can be related to the center-to-center distance of the droplets. In the example given in Fig. 6, this value is roughly 1.8 μm, which is in rough agreement with twice the droplet radii as judged from microscope pictures taken of the emulsion.

In order to analyze the data in more detail, one needs access to a theory for diffusion in these interconnected systems. One such theory was developed by Callaghan and co-workers (12). It assumes that the SGP limit

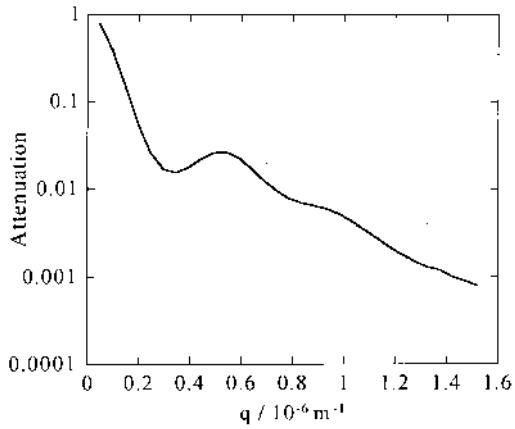

Figure 6 Diffractionlike effects in a concentrated emulsion system based on a nonionic surfactant with the composition $C_{12}E_4/C_{10}H_{22}/H_2O$ (1 wt% NaCl), (3/7/90 wt%).

described earlier is valid and it is based on a number of underlying assumptions of which pore equilibration is perhaps the most serious one. This latter assumption implies that an individual molecule in a droplet samples all of the positions in the interior of the droplet fully before it migrates to a neighboring droplet. The echo amplitude profile for such a case is given by the product of a structure factor for the single pore and a function that depends on the motion of the molecules between the pores. The pore-hopping formalism takes as input the radius of the sphere, the long-time diffusion coefficient, the center-to-center distance between the droplets, and, finally, a spread in the center-to-center distance (to account for polydispersity of the droplets). The prediction of the pore-hopping theory for the data in Fig. 6 is included as a solid line obtained with theoretical pore-to-pore distance of 1.2 μm, spread of the pore size of 0.2 μm, and the long-time diffusion coefficient $D = 9 \times 10^{-11}\,\mathrm{m^2/s}$. The agreement is not quantitative (the difference most likely owing to problems in defining a relevant structure factor for our system of polydisperse droplets), but the main features of the experimental data are certainly reproduced. A value for the lifetime of water molecule in a droplet (approximately 3 ms) was obtained from the values of the above pore-hopping parameters.

A different starting point in the analysis of the data such as the one in Fig. 6 is to make use of Brownian simulations (38). These are essentially exact within the specified model, although they do suffer from statistical uncertainties. For the present case, one lets a particle perform a random walk in a sphere with a semipermeable boundary. With a given probability, the particle is allowed to leave the droplet, after which it starts to perform a random walk in a neighboring droplet. That the approach yields peaks in the echodecay curves can be seen in Fig. 7 (38). The simulation scheme yields essentially the same kind of information as the pore-hopping theory. Thus, one obtains the droplet size and the lifetime of a molecule in the droplet (or quantities related to this, such as the permeability of the film separating the droplet).

Clearly, data such as those presented in Fig. 6 can be used to study many aspects of concentrated emulsions of which a few were exemplified earlier. It can also be used to study the evolution of the droplet size with time (recall that the method is nonperturbing) and also as a function of changes in external parameters such as temperature, which is an important variable for the properties of nonionic surfactant films.

Finally, we note that concentrated emulsions are excellent model systems in the development of the PFG methods as applied to the general class of porous systems, where the method has a great potential in providing relevant and important information.

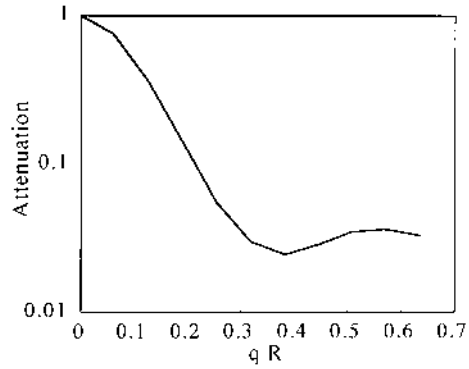

Figure 7 Brownian dynamic simulations of the echo decay at various qR for various $q = \gamma g \delta / 2\pi$ [$R = 4\,\mu m$, $P_{wall} = 0.032$ (the probability of a molecule to penetrate the film), $\Delta = 100$ ms]. The simulation scheme yields essentially the same kind of information as the pore-hopping theory. (Adapted from Ref. 38.)

V. NMR DIFFUSION STUDIES OF MULTIPLE EMULSIONS

Multiple emulsions usually refer to series of complex two-phase systems that result from dispersing an emulsion into its dispersed phase. Such systems are often referred to as water-in-oil-in-water (w/o/w) or oil-in-water-in-oil (o/w/o) emulsions, depending on the type of internal, intermediate, and continuous phase. Multiple emulsion were early recognized as promising systems for many industrial applications, such as in the process of immobilization of proteins in the inner aqueous phase (39) and as liquid membrane systems in extraction processes (40). The w/o/w emulsions have been discussed in a number of technical applications [e.g., as prolonged drug delivery systems (41–46), in the context of controlled-release formulations (47), and in pharmaceutical, cosmetic, and food applications (48)].

Multiple emulsions have a complex morphology and various important parameters for their preparation and characterization have been described (41,49). Examples are the characteristics of the w/o globules in w/o/w systems, such as their size and volume fraction, water/oil ratio inside the w/o globules, and average number and size of water droplets inside the w/o globules. The time dependence of those parameters is closely related to the stability of multiple emulsions and their morphology. Other important features are transport properties of substances encapsulated into discrete droplets and the permeability of the layer separating the internal from the external continuous phase. As was shown earlier, the NMR PFG method is a sensitive tool for studying structure and complex

dynamic phenomena, therefore, it is a promising technique in the study of multiple emulsions.

An example of possible uses of the method is demonstrated in Fig. 8, where the echo signal from the water in a w/o emulsion (panel a) and from the resulting double emulsion obtained when the original w/o emulsions is emulsified in water (panel b) are displayed (5). Also given are the resulting size distributions (panel c). The state of the water in multiple w/o/w emulsions was examined by recoding the water proton spectra (50). A narrow signal indicated water in a simple emulsion, whereas a broad signal indicated a multiple emulsion containing dispersed water.

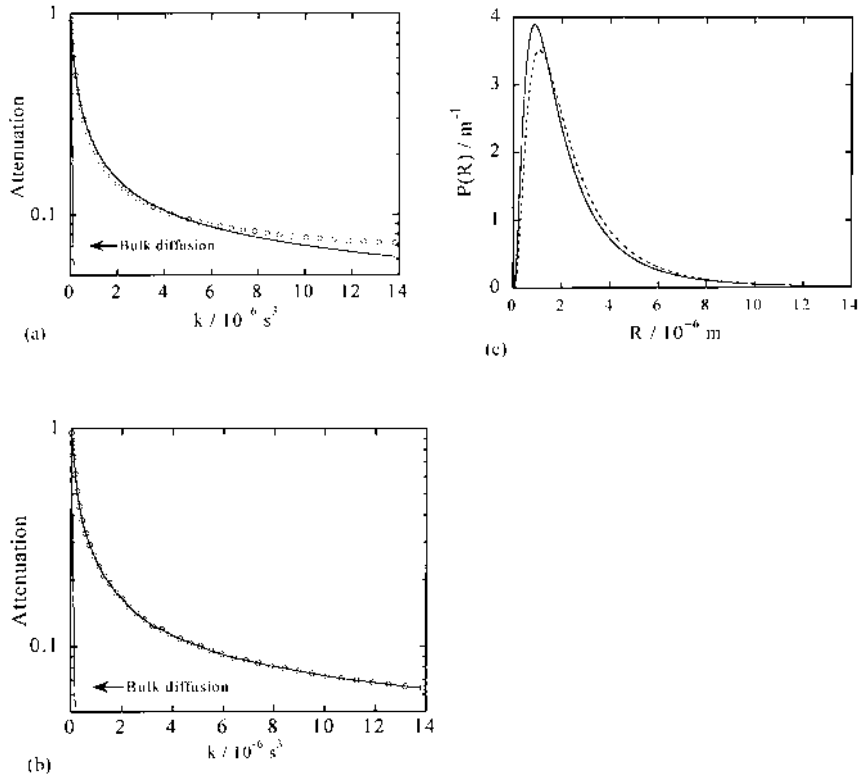

Figure 8 The echo signal from the water in a w/o emulsion (panel a), and from the resulting double emulsion obtained when the original w/o emulsions is emulsified in water (panel b). Also given in panel c are the resulting size distributions (— is w/o emulsion; --- is w/o/w emulsion). Please note that the size distribution is not normalized. (Adapted from Ref. 5.)

For studies of these complex systems, NMR is very well suited, as few other methods exist that can determine such basic properties as the state of water and the size distribution of internal emulsion droplets. In addition, the NMR PFG method may convey information about the molecular transport from emulsion droplets, a quantity that is relevant in the context of release mechanisms and rates from such emulsion carriers.

VI. DETERMINATION OF THE EMULSION COMPOSITION

Many industrial emulsion systems, such as cosmetic or pharmaceutical formulations, have well-defined compositions, whereas for other systems, the composition and nature of the ingredients may be unknown. An example of the latter is constituted by some food emulsions. The high sensitivity of the NMR experiment and ability to identify substances by their characteristic spectra may be used to quantify the emulsion composition. This method relies on the fact that the NMR spectra appears as a set of separated signals corresponding to the nuclei of interest and where the separation is due to the varying electronic environment within the molecule. The intensity of each signal, determined from the area under the signal, is proportional to the number of equivalent protons. Many emulsion systems are based on water and hydrocarbon oils, which have well-resolved lines even in quite primitive NMR spectrometers. This fact allows one to quantify the emulsion ingredients of interest (such as oil, water surfactant, or additives) without the need to separate the dispersed from the continuous phase. This quantitative characterization of emulsion systems may be particularly valuable for quality or process control, where an accurate and rapid analysis of the emulsion composition is a major requirement.

The determination of fat and water content in food emulsions with low-field NMR spectrometer requires that the relaxation time (T_2 or T_1) from each fraction are different. This situation is often at hand when the fraction of nonfat dry matter is either sufficiently large to decrease the water relaxation time, as in seeds or powders (51), or sufficiently low, as in dressings. If the discrimination is not possible, the NMR measurement should be performed before and after drying of the sample. A more sophisticated technique has been proposed in Ref. 52, which is based on the difference between the water and the fat self-diffusion. By choosing appropriate parameters of the NMR sequence, it was possible to determine both the water and the fat content in the sample.

Other methods proposed are based on the chemical shift difference between the hydroxyl group from water and methyl groups from lipid. Tellier et al. (53) demonstrated that reliable NMR determinations of water

and fat in minced meat can also be obtained under flowing conditions, a finding which suggests future on-line applications. Small variations in the water content ($< 4\%$) can be detected with a time response of less than 1 min. However, the reliability of these measurements depends on the capacity of maintaining a constant temperature in the sample. Because high-resolution NMR detects only liquid signals, temperature variations, which affect the solid/liquid ratio of the fat, induce signal fluctuation. A high-field spectrometer is not always necessary; fat and water content have also been determined with a low-field high-resolution spectrometer (54). The accuracy of the method was controlled on different meat products and cooked sausage. The main advantage of the technique is that the measurement protocol did not depend on the type of fat present. At low and medium resolution, anhydrous $CuSO_4$ can be added in order to relax the large water resonance and enhance detection of the much weaker oil resonance. This approach was used in studies of French salad dressing (55). These methods have been implemented on a magnetic resonance imaging (MRI) scanner to provide a tool to directly control the water and fat content of a bottle of French-style dressing (56). The method is a proton density projection using a spin-echo imaging sequence with the phase encode gradient turned off. The accuracy of the MRI method is within $\pm 2\%$. A MRI method for simultaneous determination of water and fat in cheese has also been proposed (57). The MRI sequence was a chemical shift selective sequence (CHESS). This sequence provides separately the fat- and water-enhanced images. Other MRI sequences have been also evaluated on dairy cream (58). The accuracy of these methods depends strongly on the main magnetic field strength, which may constitute a limitation for industrial applications. More recently, the MRI method has been developed for the control of the stability of the emulsion. When the relaxation time for oil–water emulsion is known, the volume fraction of each component phase can be calculated using

$$\frac{1}{T_{1\text{obs}}} = \frac{\phi_{\text{oil}}}{T_{1\text{oil}}} + \frac{\phi_{\text{water}}}{T_{1\text{water}}} \tag{7}$$

where φ_{oil} and φ_{water} are the volume fractions of oil and water, respectively. A fast spatially localized technique was developed for T_1 determination. Volume fractions along the profile of a 40% (v/v) oil–water emulsion were calculated several times during creaming to establish the dynamics of the process (59). This method is based on the assumption that the relaxation time of the fat and water phase was independent of the volume fraction.

The NMR characterization of emulsion composition may be quite valuable also in fundamental studies of emulsion systems and their applications. Various emulsion processing, such as creaming, solvent evaporation,

and extraction of substances by emulsions often require a quantitative analysis of the emulsion components, which can be performed with high precision using NMR techniques.

VII. ESTIMATING THE CREAMING OR SEDIMENTATION RATE

It is difficult to measure an absolute value for the creaming (or sedimentation) rate of an emulsion, as there is often a broad size distribution of the emulsion droplets. For an isolated droplet in a continuous medium, the creaming/sedimentation rate is dependent on the difference in density between the droplet and the continuous medium, the size of the droplet to the second power, and the viscosity of the continuous medium. It is obvious that different droplet sizes will give different creaming/sedimentation rates (assuming that there is a density difference between droplet and the continuous medium). We note two NMR methods that may be principally valuable in obtaining information on emulsion creaming or sedimentation. The first one is based on the quantitative analysis of the amount of dispersed phase. Emulsions containing large droplets gradually redistribute in a test tube and the creaming or sedimentation of the emulsion can be studied by determining the amount of droplet phase suspended in the emulsion at a fixed position as a function of time. This could be done directly in the NMR tube or by analyzing the amount of dispersed phase in a sample withdrawn from a fixed position of the test tube at distinct time intervals (60). Additional centrifugation of the emulsion, followed by NMR comparison of the composition of the lower and the upper fraction is a preferred method for more stable emulsions. The second method for estimating the sedimentation rate is based on flow measurements by NMR PFG. The method is sensitive to flow rates in the range of micrometers per second along the direction of the gradient of the magnetic field.

In many cases, the creaming or sedimentation occurs simultaneously with coalescence and is related to emulsion stability. In the next section, we will briefly consider the assessment of emulsion shelf life by NMR.

VIII. DETERMINATION OF EMULSION SHELF LIFE AND EMULSION STABILITY

Traditionally, emulsion stability is characterized by evaluating the droplet size distribution as a function of time and relating the results to various formulation parameters. On the basis of such studies, the thermodynamic instability of conventional emulsions is understood and well

documented (61–63). As discussed earlier, the NMR PFG is able to yield the evolution of the droplet size distribution of the same sample over time without any destruction of the sample. The change in size distribution may then be interpreted in terms of the change in the average droplet size or the total droplet area. There are two mechanisms for the decrease in the total droplet area. The first is the coalescence of two droplets involving the rupture of the film formed in the contact region of two neighboring droplets. The second process is Ostwald ripening involving the exchange of the molecules of the dispersed phase through the continuous phase. For concentrated o/w emulsions [at least the ones the present authors have investigated (64)], the permeability across the thin liquid film between the droplets is so slow that the stability is given by the film rupture mechanism. Given in Fig. 9 is the total droplet area as a function of time for a concentrated emulsion consisting of 98 wt% heptane, water, and cetyl trimethylammonium bromide (CTAB). As can be seen, there is a rapid initial decrease in the area, which levels out after about 12 h. From the initial part of the curve, the film rupture rate may be obtained, and for the data in Fig. 9, the value is 4×10^{-5} s^{-1}. At longer times, the emulsion becomes remarkable stable, and there is little or no further decrease in the total droplet area during a period of 1 year.

In some concentrated emulsions, molecular exchange between the emulsion droplets occurs on a time-scale defined by the value of Δ. This situation is at hand if the dispersed phase crosses the film by some mechanism, the detailed nature of which need not concern us here. We are then dealing with a system with permeable barriers (on the relevant

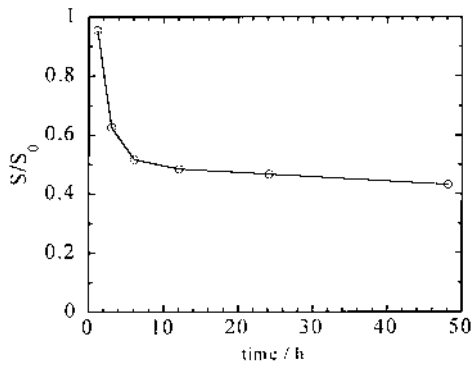

Figure 9 Decrease of the relative droplet surface area (S/S_0) with time for a highly concentrated o/w emulsion containing 98 wt% heptane and 0.4 wt% CTAB as emulsifier. S/S_0 is calculated from the droplet size distribution as obtained by the NMR self-diffusion technique. The initial slope corresponds to a film rupture rate of $J=4\times10^{-5}s^{-1}$. (Adapted from Ref. 64.)

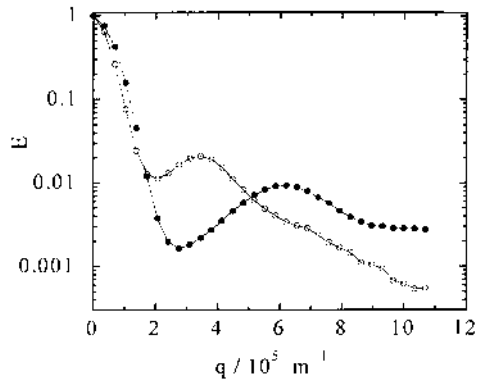

Figure 10 Normalized intensities versus q for one diffusion time ($\Delta = 50$ ms) at 2 (solid circles) and 8.5 (open circles) h after emulsion preparation. Parameters used in the experiment were $\delta = 3$ ms and a maximum gradient strength of 8.37 T/m. (Adapted from Ref. 65.)

timescale), and the system can now be regarded as belonging to the general class of porous systems. As was shown earlier, the interpretation of the NMR PFG signal in this case also gives a information on the droplet size. Given in Fig. 10 is the droplet size determined at two different instances (65), demonstrating that the stability of a concentrated emulsion with time can be conveniently followed by this method.

IX. STUDIES OF THE DISPERSED AND CONTINUOUS PHASE

A. Identification of the Dispersed Phase in Emulsions

Emulsions are formed by mixing two liquids, a process which creates discrete droplets in a continuous phase. During emulsification (e.g., by applying mechanical agitation), both liquids tend to form droplets, resulting in a complex mixture of o/w and w/o emulsions. Which of the components form the continuous phase depends on the emulsifier used because one type of the droplets is unstable and coalesce. Therefore, there is a need to identify the continuous phase in emulsion systems not only in the final emulsion system but also at short times after emulsion formation or even during the emulsification process. The NMR self-diffusion method may easily distinguish the continuous and dispersed phases based on the transport properties of its molecules. For example, molecules confined in the discrete droplets have an apparent diffusion coefficient, which is much lower than the corresponding value in the bulk phase. Molecules in the continuous phase, on the other

hand, have an apparent diffusion coefficient similar to the value in the corresponding bulk phase and this fact can be used to identify the type of continuous phase. This is particularly relevant in the case of emulsification by the phase-inversion technique (66), where a single surfactant may form either o/w or w/o emulsions depending of the formulation conditions. In many cases, the inversion of the emulsion from o/w to the w/o type (or from w/o to o/w) is a required and important step of emulsion formation. Due to its sensitivity to the transport properties of the dispersed phase, the NMR self-diffusion method is a useful tool for studying the phase-inversion process.

B. Study of the Properties of the Continuous Phase

Extensive work has been carried out in order to establish a relationship between emulsion properties and the properties of surfactant systems. The classical HLB (hydrophile–lipophile balance) concept is widely used in emulsion science to describe the balance of the hydrophilic and lipophilic properties of a surfactant at oil–water interfaces. The HLB value determines the emulsion-inversion point (EIP) at which an emulsion changes from one type to the other. This is of particular importance for nonionic surfactants that change their properties with changes in the temperature (66). Various NMR techniques have given significant contributions to the basic understanding of surfactant systems and some of those were reviewed in Ref. 8. The usefulness of NMR in studying surfactant solutions lies in the direct information they provide about the microstructure of microheterogeneous systems (8,67–71). It is beyond the scope of this chapter to summarize the use of NMR techniques to study surfactant systems, but we will present some representative examples related to emulsions.

In order to study the influence of the microstructure of the continuous phase on the stability of emulsions, two of the present authors investigated the system sodium dodecyl sulfate (SDS)/glycerolmono(2-ethylhexyl)ether/decane/brine (3 wt% NaCl) (72). In this system, emulsions of the o/w or w/o type can be made depending on the ratio between surfactant and cosurfactant. The total amount of surfactant and cosurfactant is kept constant at 5 wt%. The samples are made with equal weights of brine and decane and with a varying ratios between surfactant and cosurfactant. The emulsions in this system are made in two-phase areas of the phase diagram which for the o/w emulsions consists of an oil-rich phase and a phase of normal micelles and for the w/o emulsions consist of a water-rich phase and a micellar phase of reversed micelles. The micellar phase is the continuous medium for both types of emulsion. In order to determine the structure of the continuous medium, the emulsion samples were allowed to

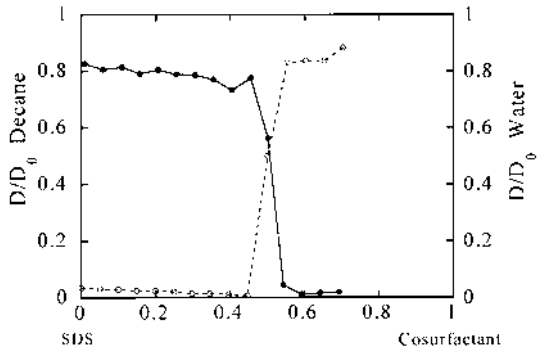

Figure 11 Microemulsion structure in the continuous phase studied by the diffusion coefficients (D) divided by the diffusion coefficients (D_0) for the neat liquid versus the relative amount of SDS in the SDS surfactant mixture. ○: decane diffusion; ●: water diffusion. (Adapted from Ref. 73.)

cream (or sediment) and the clear continuous medium was separated from each sample. These solutions were then characterized by the NMR self-diffusion method and the diffusion coefficients of both the oil and the water were determined. The result is shown in Fig. 11, where the reduced diffusion coefficients (D/D_0, where D is the actual diffusion coefficient and D_0 is the diffusion coefficient of the neat liquid at the same temperature) for the oil and the water are plotted versus the ratio between cosurfactant and surfactant. For the o/w emulsion where SDS is the only surfactant, one finds that the continuous medium consists of small spherical micelles, that the water diffusion is fast [slightly lowered relative neat water due to obstruction effects (74)], and that the oil diffusion is low and corresponds to a hydrodynamic radius of the oil swollen micelle of about 50 Å (according to Stokes law). When the cosurfactant is introduced and its amount is increased, the size of the micelles is increased, as can be inferred from the diagram by the lowered value of the reduced diffusion coefficient of the oil. Close to the three-phase area, the continuous medium is bicontinuous, as the value of the reduced diffusion coefficient is almost the same for both the oil and the water and is equal to approximately 50% of the value for the bulk liquids. When the amount of cosurfactant is increased further, one passes over to the w/o emulsion region, where the continuous medium is bicontinuous near the three-phase area and then changes to closed reversed micellar aggregates, as can be seen from the reverse in order of the magnitudes of the values of oil and water diffusion coefficients. The hydrodynamic radius of the inverse micelles is about 70 Å.

In another study (75), NMR self-diffusion measurements of the continuous oil phase show that a stable highly concentrated w/o emulsion is

formed when the continuous phase is a reverse micellar solutions, whereas unstable emulsions were formed when the continuous phase is a bicontinuous microemulsions.

C. ^{31}P-NMR of Emulsion Components

The linewidths of ^{31}P-NMR can be used to characterize the properties of phospholipids. In emulsions, the linewidths are affected by the aqueous phase pH, size, or dispersion states of particles and methods of emulsification. The hydrophilic head-group motions of emulsified egg yolk phosphatidyl-cholin (PC) and lyso PC are examined by ^{31}P-NMR to evaluate their phospholipid states and stability. The results suggest that the head-group motions of phospholipds are related to emulsion stability (76,77).

Many emulsion systems are stabilized by phospholipids that form various self-organized structures in the continuous phases. Examples are fat emulsions containing soy triacylglycerols and phospholipids that are used for intravenous feeding. Studies have shown that these emulsions contain emulsion droplets and excess phospholipids aggregated as vesicles (liposomes), which remain in the continuous phase upon separation of the emulsion droplets by ultracentrifugation. The lamellar structure of the vesicles in the supernatant was characterized by ^{31}P-NMR (78) that distinguishes lipids in the outer and inner lamellae. ^{31}P-NMR was used (79) to confirm that the resulting structures in lipid emulsions are emulsion droplets rather than lipid bilayers. The composition of the fat particles of parenteral emulsions was obtained by ^{31}P-NMR (80). Analysis of the data identified the ratio of phospholipid/triacylglycerol in various fractions of emulsion droplets separated by centrifugation. ^{31}P-NMR showed (81) that approximately 48 mol% of the phospholipid emulsifier in a model intravenous emulsion forms particles smaller than 100 nm in diameter.

^{31}P-NMR and ^{13}C-NMR may be used to study the emulsifier properties at the o/w interface. The analysis of T_1 relaxation times of selected ^{13}C and ^{31}P nuclei of β-casein in oil–water emulsions indicates (82) that conformation and dynamics of the N-terminal part of β-casein are not strongly altered at the oil–water interface. A large part of the protein was found in a random coil conformation with restricted motion with a relatively long internal correlation time.

D. Molecular Organization from Relaxation Measurements

In addition to the NMR signal intensity, values of T_1 and T_2 have been used to characterize food emulsions. Indeed, the relaxation time T_2 for the water phase is sensitive to biopolymer conformation changes through chemical

exchange mechanisms. Monitoring the water phase T_2 relaxation provides information on the effects of emulsion formation, addition of surfactants, and temperature on the biopolymer structure at the fat droplet surface. For example, large differences in the modification of T_2 induced by the formation of emulsions have been observed when adding Na-casein or β-lactoglobuline (83). Because of the initial conformation of the protein, the effect of the fat–protein interaction at the interface on the protein structure was different. The sensitivity of the relaxation time depends on the biopolymer ratio between the amount fixed at the droplet surface and the amount dispersed in the aqueous phase. If the biopolymer content in the water phase is in large excess, then the relaxation will not be sensitive to the interface. This is illustrated by the relaxation time behavior in cheese (84). In that case, the water relaxation is related to the protein/water ratio and independent of the fat content, and the T_2 relaxation time of the water phase is sensitive to the molecular and microstructural organization of the protein gel (85). The molecular structure of the protein gel induced during ripening could be monitored with T_2 relaxation measurements or T_2 maps obtained from MRI. With appropriate image analysis methods, the volume of the nonmature part and the mature part in cheese could be quantified (86) and related to sensory properties of the cheese (87,88).

The relaxation times of fat have also been studied. When the fat is in the liquid state, the relaxation time T_2 is influenced by the carbon chain length and by the degree of unsaturation (89). As many fats in food are a complex mixture of triglycerides, the NMR signal can be described by a broad distribution of relaxation times (84) and the interpretation of such behavior in food is difficult. In contrast to this situation, large changes in the longitudinal relaxation time of solid fat according to the polymorphic state have been observed in triglycerides (90). The longitudinal relaxation time was 12 s at 25°C for the polymorphic β form and decreases to 0.6 s when polymorphic α is formed. Measurement of T_1 provides a method of following the time course of the polymorphic transformation upon, for example, aging. Such variations have also been observed between fat in bulk and in emulsions for model food emulsions (83) or for real food products such as ice cream mix (91). However, because of the complexity of fat composition, the interpretation in terms of polymorphism modification is difficult.

X. DEGREE OF SOLIDIFICATION OF THE DISPERSED PHASE

Many emulsion-based formulations also contain solid particles. Typical examples in the area of food products are margarine and salad dressing.

In the food industry, the determination of the amount of solid fat is an essential part of process control. An example is the monitoring of the fat hardening in margarine after its formation as a w/o emulsion. Close control of the solid fat content (SFC) is needed to give the margarine its characteristic properties. The NMR methods used in the determination of the SFC will be briefly described in Section X.A. We conclude the chapter by discussing NMR methods in the context of emulsion stability.

A. Determination of the Solid Fat Content

The determination of the SFC content by pulsed NMR is based on the fact that the transverse magnetization of solid fat decays much faster than oil. The spin–spin relaxation time (T_2) of solid fat is about 10 μs and that of oil is about 100 ms. The NMR signal, derived from the amplitude of the FID, of partially crystallized fat after a 90° radio-frequency (RF) pulse is schematically shown in Fig. 12. The magnetization of the solid fat decays very fast. As a consequence, its contribution to the signal is far less than 0.1% of the initial value after about 70 μs. The decrease of the liquid-oil signal at this moment (70 μs) is smaller than 1% and, therefore, the signal intensity will be well proportional to the number of protons in the liquid.

Two pulsed NMR methods exist for measuring the SFC of edible oils: the direct and indirect methods. The direct method determines the SFC from the signals corresponding to the total amount of solid and liquid fat (measured at time $t \approx 0$) and the amount of liquid fat (measured at long

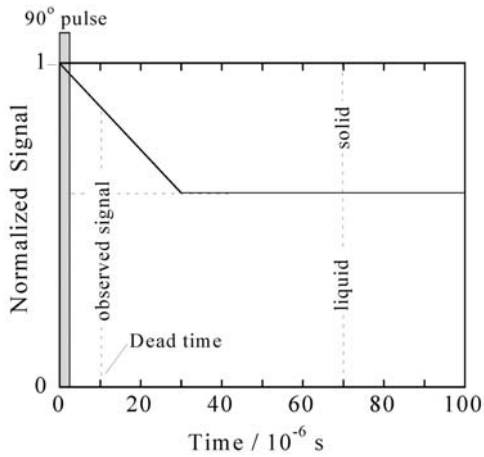

Figure 12 The NMR signal of partially crystallized fat after a 90° RF pulse.

enough time). The indirect method, determines the SFC, S_{ind}, by comparing the signal from the liquid fraction I_l with the signal I_m from completely melted fat. We have

$$S_{\text{ind}} = \frac{cI_m - I_l}{cI_m} \times 100\% \tag{8}$$

where the factor c corrects the signal for the temperature dependence of both the equilibrium magnetization and the Q-factor of the receiver coil. The correction factor $c = I_{0t}/I_{0m}$ is obtained by measuring the signals I_{0t} and I_{0m} of a reference liquid sample at both the measuring temperature and the melting temperature, respectively. The indirect method is mainly used as a reference for the direct method when the signals from both the liquid and the solid fat are processed. The indirect method is similar to the previously used continuous-wave (wide-line) technique that has some disadvantages compared to the pulsed NMR approaches. For example, saturation conditions are needed to obtain a sufficiently large signal-to-noise ratio. Even with a well-chosen reference sample, the systematic error is in the range of 1–2% (92). The wide-line analyses give only the narrow peak from the liquid fat, which should be compared to the signal of melted fat. This requires a second measurement to be performed after at least 1 h and automation of the measurement is hardly possible.

The direct method solves these problems and measures the SFC based on the processing of both the liquid and the solid signal (93). The measurement procedure may be fully automated and the percentage of solid is displayed immediately after the measurements. The measuring time is a few seconds and the SFC is determined with a standard deviation of about 0.4%. The signal can be obtained directly from the magnetization decay of the solid-fat protons and is equal to the signal immediately after the 90° pulse; see Fig. 12. Due to the dead time of the receiver, it is not possible to measure the initial signal height of solid and liquid, $s+1$, but only a signal $s'+1$ after a certain time of about 10 μs after the 90° pulse. To determine the SFC, the "true" NMR signal from solid fat, s, may be obtained from the measured signal, s', from the solid fraction multiplied with the correction factor f which depend on the T_2 of the solid fat protons. The solid fat fraction S can be expressed in terms of s' (equal to the difference between the observed and liquid signal according to Fig. 12) as

$$S = \frac{fs'}{l + fs'} \times 100\% \tag{9}$$

The correction factor $f = s/s'$ can be determined from the measured s' and the solid fraction s obtained by the indirect method [Eq. (8)] using a

reference sample. The calibration should be performed once for a series of similar samples.

The direct method is very fast and reproducible and the time for sample preparation is minimal. Only one NMR measurement is needed to obtain a SFC value.

Commercial spectrometers are available that converts the NMR signal to the percentage of SFC in fats and margarine. Examples of NMR spectrometers that are suitable for the characterization of SFC are PC100, NMS100, the Minispec from Brucker, QP20+ from Oxford Instruments, and Maran Ultra from Universal Systems. Determination of SFC by NMR is a recognized international ISO standard (94).

In contrast to calorimetric methods, NMR allows the determination of the SFC both under isothermal conditions and as a function of temperature. Consequently, many studies have been carried with the aim of understanding the effect of the fat blend on the SFC, mainly focusing on dairy fat (95–97) and cacao butter (98). The NMR method was used also for process control of the crystallization behavior (99,100). For example, effects of minor components (101), effects of surfactants (102), effects of interesterification (103,104), and effects of protein–fat interactions (102) on the crystallization of dairy fat and complex fat mixtures have been studied.

The use of the direct method and the use of calibrated standards allow for the determination of SFC expressed in mass fraction. Further assumptions made are that the hydrogen nuclei contents and relaxation properties (T_2) of the liquid and the standards are similar. For phase behavior studies, molar fractions, rather than mass fractions, of the solute in solvent are required. When all of the molecules in a sample blend are of similar molecular weight, the standard mass SFC provides a good approximation of the molar SFC. However, when the molecular weights of the blend solute and solvent differ, mass SFC can differ greatly from molar SFC (105).

The direct or indirect methods are only valid for anhydrous fat on account of the complication posed by the presence of water protons contributing to the signal. The relaxation of water is somewhat faster than that of oil, but not enough to distinguish the oil and water contributions to the signal (95). Two strategies have been proposed to tackle this problem, one is based on water suppression and the other subtracts the water phase signal from the total liquid signal. The water signal could be saturated by selecting short repetition time between the pulses (106). However, accurate results with this method assume that the liquid-fat signal is not affected by the short repetition time. In Ref. 102, it was proposed to replace water by heavy water. This method is based on the assumption that the presence of D_2O does not alter the behavior of the emulsion. Another method is to change

the relaxation time of water by adding paramagnetic ions (Cu^{2+}, Mn^{2+}), the addition of which causes the relaxation time of water to become so small that the liquid-fat signal could be estimated. This method has been used in Ref. 107 on cream, where the water phase signal was damped by adding $MnCl_2$, whereas Walstra and van Beresteyn (108) used $CuSO_4$. This method requires measurements of the water phase signal separately as well as knowledge of the exact fat fraction of the cream. Moreover, this method assumes that the water and fat signals are additive. This latter assumption has been validated in Ref. 109, where no interference between the signals were found. In order to study the influence of surfactant on ice cream mix emulsions, Barfod et al. performed two measurements: one on a water phase sample containing all water-soluble components and the other on the emulsion (110). Knowing the fat content of the mixture, the SFC could be calculated from

$$\%\mathrm{SFC} = \frac{fs \times 100}{fs + \left(l - xl_{\mathrm{H_2O}}\right)} \tag{10}$$

l represents the liquid signal, l_{H_2O} is the liquid signal from the water phase, and x is the water fraction. This latter method was recently used to study the effect fat crystallization on the behaviors of protein and lipids at a lipid–water interface (111).

As noted earlier, the determination of the SFC is based on the sampling of two points from the NMR signal: one after the dead time of the probe (11 μs) and the next one at 70 μs. This method assumes that the relaxation time of the solid part is temperature independent and independent of the fat composition when using an external reference. This assumption is not always valid. For example, the precise analysis of the free-induction signal of milk fat at 5°C shows that an intermediate phase, characterized by a relaxation time T_2^* varying in the 50–250-μs range, could be detected (112). This intermediate phase represents about 4% of the entire fat content and, consequently, it should be considered when absolute values of SFC are required. An alternative is to analyze the complete NMR signal. This approach provides a precise determination of the relaxation time of the solid phase and the signal intensity is deduced without the need to correct for probe dead time. This method has been successfully applied on fat blends (113), on model food emulsions (83,114), on cheese (84) and ice cream mix (91).

The NMR method for determining SFC has been implement on a MRI scanner (115). The procedure to quantify the rate of crystallization is essentially the same as for the indirect method in spectroscopic NMR experiments. The method has been used to study the fat signal intensity

from pure chocolate bars as a function of the cooling rate (116). The variation in the signal intensity was interpreted in terms of variations in the solid/liquid ratio of the cacao butter; hence, the existence of different polymorphic forms in the two samples was suggested. Differential Scanning Calorimetry (DSC) experiments confirmed this interpretation. Applied on adipose tissues from pig carcasses, a strong linear relationship was found between the SFC and the fat composition and this allowed for an accurate mapping of the solid/liquid ratio in animal subcutaneous adipose tissues and in intermuscular fat tissues from different pieces (117). The primary information obtained from MRI studies of lipid crystallization is the crystal growth rate (115,118). Oil-weighted MR images were obtained using a T_1-weighed spin-echo sequence. The water signal was attenuated by using a small delay between the RF pulses. The crystallization dynamics was quantified from localized spectroscopy using a stimulated echo-pulse sequence. The method was then evaluated on model system both in bulk and in emulsion system. The results show that the rate of lipid crystallization differs significantly from bulk to the oil–water emulsion state and that difference is dependent on the nature of the triglycerides (115). From NMR and MRI studies, the crystal growth has been empirically modeled and revealed a significant trilaurin-location dependence, confirming that the rates of the nucleation processes were affected both by the concentration of trilaurin and the heat transfer properties of the sample and vessel (118).

B. Studies of the Emulsion Stability

It was demonstrated (119,120) that pulsed NMR may be used to measure the extent of oil solidification during cooling of oil-in-water emulsions. Pulsed proton NMR can distinguish between the oil and aqueous phases because of the large differences between the relaxation times of oil and water protons. On cooling, the NMR signal obtained for the aqueous phase is relatively small compared to the oil phase during the entire cooling cycle. For example, the water signal was approximately 10 times lower than the water signal for o/w emulsion containing approximately 50% hydrogenated oil (121). When the lipid phase containing the lipophilic emulsifier is cooled, the NMR signal decreases as the sample solidifies. The NMR signals from the different types of protons of the emulsion system are approximately additive (the sum of the aqueous and oil phases). In practice, the signal obtained for the supercooled emulsion is always larger than expected from a mixture with a solid fat and water, indicating that emulsification has had an inhibiting effect on fat solidification. The dispersion of fat into small droplets suppresses the rate of solidification under supercooling due to

nucleation phenomena in confined emulsion droplets (122–124). The extent of solidification at supercooling is high for very large emulsion droplets and correlates with a low emulsion stability. Unstable emulsions show little supercooling, but those that are relatively stable to creaming and phase separation are resistant to oil solidification. The greater the degree of dispersion, the slower the rate of phase separation. A correlation was made between the emulsion stability and the NMR signal from the emulsion when compared to the NMR signal from the fat and water phase alone (121). A parameter called "percent interaction" was derived from the NMR signal (120), the value of which correlated well with actual resistance of the emulsion to creaming and phase separation during storage. For example, the NMR signals from an emulsion and its corresponding fat phases were determined for an emulsion containing 48% hydrogenated oil, 1% acetylated monoglyceride (a 49% total fat phase), 1% Tween-20, and 50% water (a 51% aqueous phase) (121) as follows:

Fat phase signal	$71.5 \times 0.49 = 35.0$
Aqueous phase signal	$7.51 \times 0.51 = 3.8$
Expected emulsion signal	38.8
Observed emulsion signal	41.5

The "interaction percentages" (Int%) were calculated using

$$\text{Int\%} = \left(\frac{s_1 + l + w}{s + w} - 1 \right) \times 100\% \tag{11}$$

where the observed emulsion signal ($s_1 + l + w$) corresponding to the signal from the solidified fat fraction, s_1, and not solidified fat, l, and water, w, was compared to the expected emulsion signal ($s + w$) corresponding to solid fat and water.

An emulsion is considered to be relatively stable if the observed NMR is more than 30% larger compared to the sum of the NMR signal from corresponding bulk water and oil (121). Pulsed NMR cooling curve measurements on emulsions offer an improved method for prediction of emulsion stability. By using a flow-through cell in the NMR magnet, the rate and extent of phase separation was measured accurately (120). The method is useful in selection of optimum types and levels of emulsifiers for each system (119). NMR measurements can also assist in optimizing surfactant blends to obtain stable emulsion. At the optimum emulsion formulation for a particular oil, the "interaction percentage" will be at a maximum, which indicates higher emulsion stability.

XI. CONCLUSIONS

In the above sections, we have presented various applications of the NMR technique in the study of emulsions. NMR is a versatile spectroscopic technique. This is also reflected in the span of questions pertaining to various aspects of emulsions that can be addressed with the NMR technique. The topics covered there include the determination of droplet size distributions, aspects of emulsion stability, crystallization of fat, and determination of fat and water contents in food emulsions.

It seems quite clear that emulsions will become increasingly important in more specialized applications in the future. In such applications, the demands for accurate design of properties of the emulsion systems, process, and quality control will be a major challenge. As should be clear from the above, NMR will become increasingly important in this regard. Controlled delivery of drugs as well as the use in the administration of pesticides is two examples of emulsion technology that will require accurate and reproducible characterization.

Due to its insensitivity to the physical nature of the sample and to its nonperturbing character, it seems likely that different NMR methods will find increasing use in studies of emulsions that are important in various types of food.

ACKNOWLEDGMENT

The work was financially supported by the Swedish Board for Industrial and Technical Development (NUTEC).

REFERENCES

1. A. Kabalnov and H. Wennerström, *Langmuir* 12, 276–292 (1996).
2. P. T. Callaghan, *Principles of Nuclear Magnetic Resonance Microscopy*, Clarendon Press, Oxford, 1991.
3. R. R. Ernst, G. Bodenhausen, and A. Wokaun, *Principles of Nuclear Magnetic Resonance in One and Two Dimensions,* Oxford University Press, Oxford, 1987.
4. D. Canet, *Nuclear Magnetic Resonance. Concepts and Methods,* Wiley, Chichester, 1996.
5. I. Lönnqvist, B. Håkansson, B. Balinov, and O. Söderman. *J. Colloid Interf. Sci.* 192, 66–73 (1996).
6. P. T. Callaghan, C. M. Trotter, and K. W. Jolley, *J. Magn. Reson.* 37, 247–259 (1980).
7. P. Stilbs, *Prog. Nucl. Magn. Reson. Spectrosc.* 19, 1–45 (1987).

8. O. Söderman and P. Stilbs, *Prog. Nucl. Magn. Reson. Spectrosc.* 26, 445–482 (1994).
9. E. O. Stejskal and J. E. Tanner, *J. Chem. Phys.* 42, 288–292 (1965).
10. J. E. Tanner, Thesis, University of Wisconsin–Madison, 1966.
11. P. T. Callaghan and A. Coy, in *NMR Probes of Molecular Dynamics*, (P. Tycko, ed.), Kluwer Academic, Dordrecht, 1993.
12. P. T. Callaghan, A. Coy, T. P. J. Halpin, D. MacGowan, J. K. Packer, and F. O. Zelaya. *J. Chem. Phys.* 97, 651–662 (1992).
13. A. V. Barzykin, *Phys. Rev. B* 58, 14,171–14,174 (1998).
14. S. L. Codd and P. T. Callaghan. *J. Magn. Reson.* 137, 358–372 (1999).
15. J. Kärger and W. Heink, *J. Magn. Reson.* 51, 1–7 (1983).
16. J. E. Tanner and E. O. Stejskal, *J. Chem. Phys.* 49, 1768–1777 (1968).
17. B. Balinov, B. Jönsson, P. Linse, and O. Söderman, *J. Magn. Reson. A* 104, 17–25 (1993).
18. D. C. Douglass and D. W. McCall, *J. Phys. Chem.* 62, 1102 (1958).
19. C. H. Neuman, *J. Chem. Phys.* 60, 4508–4511 (1974).
20. J. S. Murday and R. M. Cotts, *J. Chem. Phys.* 48, 4938–4945 (1968).
21. B. Balinov, O. Söderman, and T. Wärnheim, *J. Am. Oil Chem. Soc.* 71, 513–518 (1994).
22. B. Balinov, O. Urdahl, O. Söderman, and J. Sjöblom, *Colloids Surfaces* 82, 173–181 (1994).
23. P. T. Callaghan, K. W. Jolley, and R. Humphrey, *J. Colloid Interf. Sci.* 93, 521–529 (1983).
24. X. Li, J. C. Cox, and R. W. Flumerfelt, *AIChE J.* 38, 1671–1674 (1992).
25. I. Lönnqvist, A. Khan, and O. Söderman, *J. Colloid Interf. Sci.* 144, 401–411 (1991).
26. K. J. Packer and C. Rees, *J. Colloid Interf. Sci.* 40, 206–218 (1972).
27. J. C. van den Enden, D. Waddington, H. Van Aalst, C. G. Van Kralingen, and K. J. Packer, *J. Colloid Interf. Sci.* 140, 105–113 (1990).
28. L. Ambrosone, A. Ceglie, G. Colafemmina, and G. Palazzo, *J. Chem. Phys.* 110, 797–804 (1999).
29. L. Ambrosone, A. Ceglie, G. Colafemmina, and G. Palazzo, *J. Chem. Phys.* 107, 10,756–10,763 (1997).
30. P. Stilbs and M. Moseley, *J. Magn. Reson.* 31, 55–61 (1978).
31. L. Ambrosone, G. Colafemmina, M. Giustini, G. Palazzo, and A. Ceglie, *Prog. Colloid Polym. Sci.* 112, 86–88 (1999).
32. G. Roudaut, D. van Dusschoten, H. van As, M. A. Hemminga, and M. Lemeste, *J. Cereal Sci.* 28, 147–155 (1998).
33. M. M. Britton and P. T. Callaghan, *J. Texture Studies* 31, 245–255 (2000).
34. K. J. Lissant, *J. Colloid Interf. Sci.* 22, 462–468 (1966).
35. H. M. Princen, *J. Colloid Interf. Sci.* 91, 160–175 (1983).
36. P. T. Callaghan, A. Coy, D. MacGowan, K. J. Packer, and F. O. Zelaya, *Nature (London)* 351, 467–469 (1991).
37. R. Pons, I. Carrera, P. Erra, H. Kunieda, and C. Solans, *Colloids Surfaces A* 91, 259–266 (1994).

38. B. Balinov, P. Linse, and O. Söderman, *J. Colloid Interf. Sci.* 182, 539–548 (1996).
39. R. H. Engel, S. J. Riggi, and M. J. Fahrenbach, *Nature* 219, 856–857 (1968).
40. N. N. Li and A. L. Shrier, in *Recent Developments in Separation Science* (N. N. Li, ed.), Chemical Rubber Co., Cleveland, OH, 1972.
41. S. Matsumoto, in *Nonionic Surfactants* (M. Schick, ed.), Marcel Dekker, New York, 1987.
42. P. J. Taylor, C. L. Miller, T. M. Pollack, F. T. Perkins, and M. A. Westwood, *J. Hyg.* (*London*) 67, 485–890 (1969).
43. L. A. Elson, B. C. Mitchlev, A. J. Collings, and R. Schneider, *Rev. Eur. Etudes Clin. Biol.* 15, 87–90 (1970).
44. C. J. Benoy, L. A. Elson, and R. Schneider, *Br. J. Pharmacol.* 45, 135–136 (1972).
45. A. F. Brodin, D. R. Kavaliunas, and S. G. Frank, *Acta Pharm. Suec.* 15, 1–12 (1978).
46. D. Whitehill, *Chem. Drug* 213, 130–135 (1980).
47. R. K. Owusu, Z. Qinhong, and E. Dickinson, *Food Hydrocolloids* 6, 443–453 (1992).
48. E. Dickinson, J. Evison, and R. K. Owusu, *Food Hydrocolloids* 5, 481–485 (1991).
49. M. Frenkel, R. Shwartz, and N. Garti, *J. Colloid Interf. Sci.* 94, 174–178 (1983).
50. A. Rabaron, P. A. Rocha-Filho, C. Vaution, and M. Seiller, Study and demonstration of multiple w/o/w emulsions by nuclear magnetic resonance, in *Fifth International Congress on the Technology of Pharmaceuticals*, 1989.
51. R. E. Hester and D. E. C. Quine, *J. Dairy Res.* 44, 125–130 (1977).
52. H. Berg, Determination of fat and water content in meat with NMR, in *Fifth International Conference on Applications of Magnetic Resonance in Food Science*, 2000.
53. C. Tellier, M. Trierweiler, J. Lejot, and G. J. Martin, *Analusis* 18, 67–72 (1990).
54. J. P. Renou, A. Briguet, P. Gatellier, and J. Kopp, *Int. J. Food Sci. Technol.* 22, 169–172 (1987).
55. P. Fairbrother and D. N. Rutledge, *Analusis* 21, 113–117 (1993).
56. J. R. Heil, W. E. Perkins, and M. J. McCarthy, *J. Food Sci.* 55, 763 (1990).
57. R. Ruan, K. Chang, P. L. Chen, R. G. Fulcher, and E. D. Bastian, *J. Dairy Sci.* 80, 9–15 (1998).
58. S. L. Duce, M. H. G. Amin, M. A. Horsfield, M. Tyszka, and L. D. Hall, *Int. Dairy J.* 5, 311–319 (1995).
59. R. J. Kauten, J. E. Maneval, and M. J. McCarthy, *J. Food Sci.* 56, 799–801 (1991).
60. M. Gangoda, B. M. Fung, and E. A. O'Rear, *J. Colloid Interf. Sci.* 116, 230–236 (1987).
61. C. Washington, *Int. J. Pharm.* 66, 1–21 (1990).
62. J. Boyd, C. Parkinson, and P. Sherman, *J. Colloid Interf. Sci.* 41, 359–370 (1972).
63. N. Weiner, *Drug Dev. Ind. Pharm.* 12, 933–951 (1986).

64. O. Söderman and B. Balinov, in *Emulsions and Emulsion Stability* (J. Sjöblom, ed.), Marcel Dekker, New York, 1996.
65. B. Håkansson, R. Pons, and O. Söderman, *Langmuir* 15, 988–991 (1999).
66. L. Marszall, in *Nonionic Surfactants* (M. Schick, ed.), Marcel Dekker, New York, 1987.
67. B. Lindman, O. Söderman, and H. Wennerström, in *Novel Techniques to Investigate Surfactant Solutions* (R. Zana, ed.), Marcel Dekker, New York, 1987.
68. B. Balinov, U. Olsson, and O. Söderman, *J. Phys. Chem.* 95, 5931–5936 (1991).
69. B. Lindman and P. Stilbs, in *Microemulsion Systems* (H.L. Rosano and M. Clausse, eds.), Marcel Dekker, New York, 1987.
70. B. Lindman, K. Shinoda, U. Olsson, D. Andersen, G. Karlström, and H. Wennerström, *Colloids Surfaces* 38, 205–224 (1989).
71. A. Khan, in *Specialist Periodical Reports, Nuclear Magnetic Resonance* (G. A. Webb, ed.), The Royal Society of Chemistry, Cambridge, 1993.
72. K. Shinoda, H. Kunieda, T. Arai, and H. Saijo, *J. Phys. Chem.* 88, 5126–5129 (1984).
73. O. Söderman, I. Lönnqvist, and B. Balinov, in *Emulsions—A Fundamental and Practical Approach*, (J. Sjöblom, ed.), Kluwer Academic, Dordrecht, 1992.
74. B. Jönsson, H. Wennerström, P. Nilsson, and P. Linse, *Colloid Polym. Sci.* 264, 77 (1986).
75. C. Solans, R. Pons, S. Zhu, H. T. Davis, D. F. Evans, K. Nakamura, and H. Kunieda, *Langmuir* 9(6), 1479–1482 (1993).
76. K. Chiba and M. Tada, *Nippon Nogei Kagaku Kaishi* 62, 859–865 (1988).
77. K. Chiba and M. Tada, *Agric. Biol. Chem.* 53, 995–1001 (1989).
78. M. Rotenberg, M. Rubin, A. Bor, D. Meyuhas, Y. Talmon, and D. Lichtenberg, *Biochim. Biophys. Acta* 1086, 265–272 (1991).
79. J. Drew, A. Liodakis, R. Chan, H. Du, M. Sadek, R. Brownlee, and W. H. Sawyer, *Biochem. Int.* 22, 983–992 (1990).
80. J. Férézou, T. L. Nguyen, C. Leray, T. Hajri, A. Frey, Y. Cabaret, J. Courtieu, C. Lutton, and A. C. Bach, *Biochim. Biophys. Acta* 1213, 149–158 (1994).
81. K. Westesen and T. Wehler, *J. Pharmaceut. Sci.* 82, 1237–1244 (1993).
82. L. C. ter Beek, M. Ketelaars, D. C. McCain, P. E. Smulders, P. Walstra, and M. A. Hemminga, *Biophys. J.* 70, 2396–2402 (1996).
83. F. Mariette, S. Querangal, M. Cambert, C. C. Lopez, and A. Riaublanc, in Protein structural changes ar the O/W interface emulsion studied by NMR relaxometry, *Fifth International Conference on Applications of Magnetic Resonance in Food Science*, 2000.
84. B. Chaland, F. Mariette, P. Marchal, and J. de Certaines, *J. Dairy Res.* 67, 609–618 (2000).
85. B. Chaland, Thesis, University of Rennes, France, 1999.
86. B. Chaland, F. Mariette, P. Marchal, and J. de Certaines, Macro structural and morphological changes during soft cheese ripening by MRI, in *Fifth International Conference on Applications of Magnetic Resonance in Food Science*, 2000.

87. F. Mariette, G. Collewet, P. Marchal, and J. M. Franconi, in *Advances in Magnetic Resonance in Food Science* (P. Belton, B. Hills, and G. A. Webb, eds.), The Royal Society of Chemistry, Cambridge, 1999.
88. F. Mariette, G. Collewet, P. Fortier, and J. M. Soulie, in *Magnetic Resonance in Food Science—A View to the Future* (G. A. Webb, P. Belton, A. M. Gil, and I. Delgadillo, eds.), The Royal Society of Chemistry, Cambridge, 2001.
89. D. J. LeBotlan and I. Helie, *Analusis* 22, 108–113 (1994).
90. I. J. Colquhoun and A. Grant, Solid State NMR spectrocopy of fats, in *Eurofood Chem V*, 1989.
91. T. Lucas, S. Dominiawsyk, F. Mariette, and G. Alvarez, ^{1}H NMR assessment of water behaviour in ice cream, in *Engineering Food, Eighth ICEF International Conference Proceedings*, 2000.
92. A. J. Haighton, K. van Putte, and L. F. Vermaas, *J. Am. Oil Chem. Soc.* 49, 153–156 (1972).
93. K. van Putte and J. van den Enden, *J. Phys. E: J. Sci. Instrum.* 6, 910–912 (1973).
94. ISO 8292: 1991, Animal and vegetable fats and oils: determination of solid fat content, pulsed nuclear magnetic resonance method, International Organization for Standardization (1991).
95. B. K. Mortensen, in *Developments in Dairy Chemistry — 2. Lipids* (P. F. Fox, ed.), Applied Science, London, 1983.
96. N. M. Barfod, in *Characterization of Food: Emerging Methods* (A. G. Gaonkar, ed.), Elsevier, New York, 1995.
97. M. L. Herrera, M. D. Gatti, and R. W. Hartel, *Food Res. Int.* 32, 289–298 (1999).
98. H. K. Leung, G. R. Anderson, and P. J. Norr, *J. Food Sci.* 50, 942–945 (1985).
99. K. E. Kaylegian and R. C. Lindsay, *J. Dairy Sci.* 75, 3307–3317 (1992).
100. B. Breitschuh and E. J. Windhab, *J. Am. Oil Chem. Soc.* 73, 1603–1610 (1996).
101. A. J. Wright, R. W. Hartel, S. S. Narine, and A. G. Marangoni, *J. Am. Oil Chem. Soc.* 77, 463–475 (2000).
102. N. M. Barfod and N. Krog, *J. Anal. Org. Chem. Soc.* 64, 112–119 (1987).
103. A. G. Marangoni and D Rousseau, *J. Am. Oil Chem. Soc.* 75, 1265–1271 (1998).
104. D. Rousseau, K. Forestiere, A. R. Hill, and A. G. Marangoni, *J. Am. Oil Chem. Soc.* 73, 963–972 (1996).
105. A. G. Marangoni, A. J. Wright, S. S. Narine, and R. W. Lencki, *J. Am. Oil Chem. Soc.* 77, 565–567 (2000).
106. S. Shanbhag, M. P. Steinberg, and A. I. Nelson, *J. Am. Oil Chem. Soc.* 48, 11 (1971).
107. E. G. Samuelson and J. Vikelsoe, *Milchwissenschaft* 26, 621–625 (1971).
108. P. Walstra and E. C. H. Van Beresteyn, *Netherlands Milk Dairy J.* 29, 36–65 (1975).
109. M. A. J. S. Van Boekel, *J. Am. Oil Chem. Soc.* 51, 316–320 (1974).
110. N. M. Barfod, N. Krog, G. Larsen, and W. Buchheim, *Fat Sci. Technol.* 1, 24–29 (1991).

111. T. Sugimoto, T. Mori, J. Mano, T. A. Mutoh, Y. Shiinoki, and Y. Matsumura, *J. Am. Oil Chem. Soc.* 78, 183–188 (2001).
112. D. Le Botlan and I. Helie, *Anal. Chim. Acta* 311, 217–223 (1995).
113. J. Van Duynhoven, I. Dubourg, G. J. Goudappel, and E. Roijers, *J. Am. Oil Chem. Soc.* 79, 383–388 (2002).
114. D. Le Botlan, J. Wennington, and J. C. Cheftel, *J. Colloid Interf. Sci.* 226, 16–21 (2000).
115. C. Simoneau, M. J. McCarthy, R. J. Kauten, and J. B. German, *J. Anal. Org. Chem. Soc.* 68, 481–487 (1991).
116. S. L. Duce, T. A. Carpenter, and L. D. Hall, *Lebensm. Wiss. Technol.* 23, 545–590 (1990).
117. A. Davenel, P. Marchal, A. Riaublanc, and G. Gandemer, in *Advances in Magnetic Resonance in Food Science* (P. Belton, B. Hills, G. A. Webb, eds.), The Royal Society of Chemistry, Cambridge, 1999.
118. S. Ozilgen, C. Simoneau, J. B. German, M. J. McCarthy, and D. S. Reid, *J. Sci. Food Agric.* 61, 101–108 (1993).
119. J. Trumbetas, J. A. Fioriti, and R. J. Sims, *J. Am. Oil Chem. Soc.* 53(12), 722–726 (1976).
120. J. Trumbetas, J. A. Fioriti, and R. J. Sims, *J. Am. Oil Chem. Soc.* 55(2), 248–251 (1978).
121. J. L. Cavallo and D. L. Chang, *Chem. Eng. Prog.* 86, 54–59 (1990).
122. D. Turubull, *J. Chem. Phys.* 20, 411 (1952).
123. J. P. C. Cordiez, G. Grange, and B. Mutaftschiev, *J. Colloid Interf. Sci.* 85, 431–441 (1982).
124. D. Clausse, in *Encyclopedia of Emulsion Technology*, (P. Becher, ed.), Marcel Dekker, New York, 1985.